PLANETARY SCIENCE

# Discovery of diffuse aurora on Mars

N. M. Schneider,[1]* J. I. Deighan,[1] S. K. Jain,[1] A. Stiepen,[1] A. I. F. Stewart,[1] D. Larson,[2] D. L. Mitchell,[2] C. Mazelle,[3,4] C. O. Lee,[2] R. J. Lillis,[2] J. S. Evans,[5] D. Brain,[1] M. H. Stevens,[6] W. E. McClintock,[1] M. S. Chaffin,[1] M. Crismani,[1] G. M. Holsclaw,[1] F. Lefevre,[7] D. Y. Lo,[8] J. T. Clarke,[9] F. Montmessin,[8] B. M. Jakosky[1]

**Planetary auroras reveal the complex interplay between an atmosphere and the surrounding plasma environment. We report the discovery of low-altitude, diffuse auroras spanning much of Mars' northern hemisphere, coincident with a solar energetic particle outburst. The Imaging Ultraviolet Spectrograph, a remote sensing instrument on the Mars Atmosphere and Volatile Evolution (MAVEN) spacecraft, detected auroral emission in virtually all nightside observations for ~5 days, spanning nearly all geographic longitudes. Emission extended down to ~60 kilometer (km) altitude (1 microbar), deeper than confirmed at any other planet. Solar energetic particles were observed up to 200 kilo–electron volts; these particles are capable of penetrating down to the 60 km altitude. Given minimal magnetic fields over most of the planet, Mars is likely to exhibit auroras more globally than Earth.**

Auroras are hallmarks of energetic particle deposition in planetary upper atmospheres. They can be used to understand composition, structure, and chemistry of the target atmosphere, as well as the energy and flux of particles striking the atmosphere. Auroral emission in planetary atmospheres can be caused by a number of incident particle populations, energized via a variety of processes. Distinguishing between the various auroral phenomena is best achieved via a combination of observations of both the precipitating particles and the emitted photon radiation. Auroras at Earth are well studied by these complementary means (*1*).

At least three distinct types of aurora are present in Earth's atmosphere (*2*). The brightest and most widely discussed is called "discrete aurora," in reference to its spatial confinement within auroral ovals roughly encircling Earth's magnetic poles. This type of aurora is powered by some combination of parallel electric fields and plasma waves that accelerate the precipitating particles. A second type of aurora can occur equatorward of the auroral zones and is caused by particles locked deeper in Earth's magnetic field. Named "diffuse aurora" or "drizzle," it occurs over much wider spatial ranges, without discernible patterns or structure. It also differs from discrete aurora in that it arises from particles scattered into Earth's atmosphere without acceleration. A third type of aurora occurs poleward of the auroral ovals, again from particles (in this case, solar wind electrons) precipitating into the atmosphere without local acceleration (*3*). Though also morphologically diffuse, this type of aurora is called "polar rain aurora" so as to differentiate this type from the diffuse aurora described above. Normally, both forms of morphologically diffuse aurora are fainter than discrete auroras, owing to their lower particle flux and energy. In all three cases, these terrestrial auroras are confined to the polar region with an emission peak in the upper atmosphere or thermosphere.

The collision of energetic particles with planetary atmospheres is nearly unavoidable, so auroras are a widespread planetary phenomenon. Auroras have been detected at all planets with substantial atmospheres, as well as at some moons with atmospheres. These planetary auroras are either discrete, in cases with intrinsic magnetic fields, or diffuse, in cases without.

Mars is an interesting intermediate case, for which parts of the planet retain remanent magnetism that was locked in the crust about 4 billion years ago, whereas the rest of the planet has a negligible intrinsic magnetic field (*4*). Discrete auroras were detected in regions of strong crustal magnetic fields by the SPICAM (Spectroscopy for Investigation of Characteristics of the Atmosphere of Mars) instrument on the European Space Agency's Mars Express orbiter (*5*–*7*). The emission appeared in patches that were tens of kilometers across at altitudes around 130 km. Further analysis (*8*) revealed a total of 20 instances of auroral patches during 10 years of intermittent SPICAM observations. Auroral excitation was attributed to the precipitation of electrons, typically up to 1 keV, likely accelerated by parallel electric fields analogous to Earth's discrete aurora (*9*, *10*).

Discrete auroras provide concrete evidence of particle precipitation into the martian nightside atmosphere in localized regions, and the likely effects of more global precipitation of charged particles during both quiet and solar storm periods have also been considered (*11*–*13*). However, auroral emission caused by global precipitation had never been discussed. Thus, it remained uncertain whether auroral processes were primarily local effects in specific small-scale regions or a widespread planetary process affecting upper atmospheric chemistry, energy balance, and loss processes on a more global scale.

## Observations

The Mars Atmosphere and Volatile Evolution (MAVEN) spacecraft entered Mars' orbit in September 2014, on a mission to study the behavior of the upper atmosphere and the escape of its constituent gases to space (*14*). MAVEN orbits Mars on a 4.5-hour elliptical orbit, with a closest approach to Mars' surface at the periapse, with a distance of ~150 km. MAVEN carries nine instruments optimized for the study of the Mars atmosphere, as well as the drivers that control its behavior. The majority of instruments are used to study the electromagnetic fields and particle environment that surround and collide with Mars' upper atmosphere.

MAVEN also carries a remote sensing instrument for the study of Mars' upper atmosphere: the Imaging Ultraviolet Spectrograph (IUVS) (*15*). The instrument captures reflectance and emission spectra of the planet and its atmosphere in the far-ultraviolet (FUV) (110 to 190 nm) and mid-UV (MUV) (180 to 340 nm) regions, ideal for recording well-known atmospheric emissions from $CO_2$ and its dissociation and ionization products. The instrument is mounted on an articulated payload platform (APP) that can orient IUVS's field of regard relative to Mars, depending on spacecraft location, orientation, and desired viewing geometry. At the periapse, the APP orients IUVS to look to the side of spacecraft motion, allowing IUVS to use a scan mirror to repeatedly map out the vertical structure of the emitting layers while the spacecraft travels ~90° around the planet. IUVS uses different observing modes in other parts of the orbit, but no auroral emissions have yet been detected in those modes.

We report on periapse observations for 42 orbits between orbit 382 (9 December 2014) and orbit 453 (23 December 2014), with gaps during data downlinks, observations by other instruments, and instrument protection commanding. Data were corrected for detector dark current and scaled according to intensity calibration with UV-bright stars, scaled by instrument geometric factors appropriate for extended source observations (*16*). The MUV data presented herein carry a systematic uncertainty of 30%. The data used in this study, archived with the Planetary Data System, can be identified by the orbit numbers above, the label "periapse" in the filename, and "v02_r01" as a version and revision identifier. Cleaned spectra and vertical profiles of individual emissions were obtained through multiple linear regression fits of independent spectral components (*17*), accounting for molecular bands, atomic lines, and reflected solar spectrum background, as

[1]Laboratory for Atmospheric and Space Physics, University of Colorado, Boulder, Boulder, CO 80303, USA. [2]Space Sciences Lab, University of California, Berkeley, Berkeley, CA 94720, USA. [3]Institut de Recherche en Astrophysique et Planétologie (IRAP), CNRS, Toulouse, France. [4]University Paul Sabatier, IRAP, CNRS, Toulouse, France. [5]Computational Physics, Inc, Springfield, VA 22151, USA. [6]Space Science Division, Naval Research Laboratory, Washington, DC 20375, USA. [7]Laboratoire Atmosphères, Milieux, Observations Spatiales, Institut Pierre Simon Laplace, Guyancourt, France. [8]Lunar and Planetary Laboratory, University of Arizona, Tucson, AZ 85721, USA. [9]Center for Space Physics, Boston University, Boston, MA 02215, USA.
*Corresponding author. E-mail: nick.schneider@lasp.colorado.edu

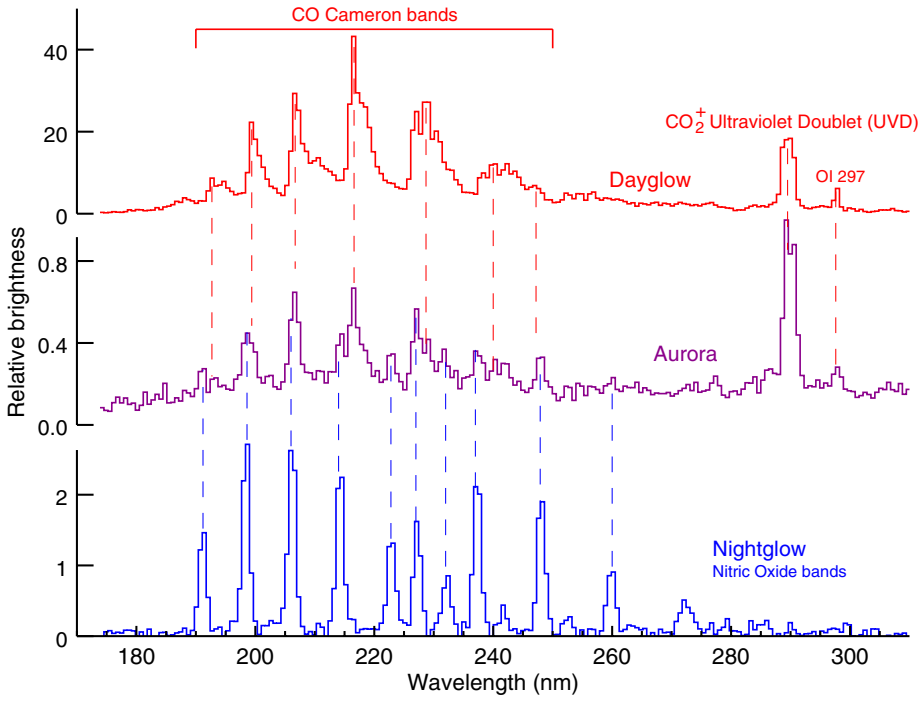


**Fig. 1. Three types of Mars spectra observed by IUVS.** The top spectrum shows three dayglow emission features from the ionization and dissociation products of $CO_2$ created by solar EUV radiation (*19*). The bottom spectrum shows a nightside spectrum under conditions where nitric oxide nightglow (*38*, *39*) is produced by atmospheric chemistry; no other emissions are present. Dotted lines from peaks in the top and bottom spectra show that the middle spectrum from the nightside is a combination of features seen in dayglow and nightglow, indicating that particle precipitation is responsible for creating the spectral features of dayglow on the nightside. The differences at 289 nm are most pronounced, as the nitric oxide and Cameron bands have considerable overlap. Spectra were obtained during orbits 114 (top), 437 (middle), and 387 (bottom). OI refers to emission from neutral oxygen.

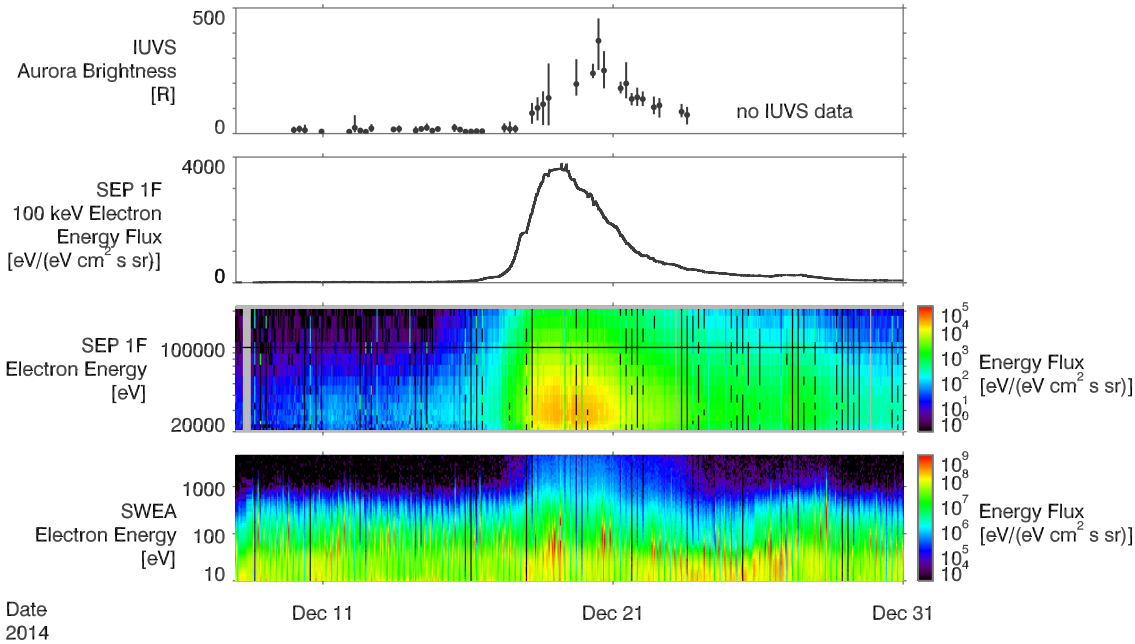


**Fig. 2. Time series for auroral emissions and precipitating electron populations.** UVD brightnesses measured by IUVS (**top panel**) are compared to the precipitating electrons measured by SEP (**middle panels**) and SWEA (**bottom panel**). The upper SEP panel plots the flux at 100 keV, whereas the lower panel displays all energies. The rise in auroral emission is well correlated with the arrival of the solar energetic particles. Auroral brightnesses in the top panel are averages for entire periapse passes, over the altitude range from 60 to 100 km and over five limb scans spanning 35° of latitude. The maximum and minimum values within each periapse pass are also shown, indicating the intrinsic variability. Emission brightnesses are given in units of rayleighs (R).

well as instrumental resolution and instrumental backgrounds (*18*).

## Results

Three types of MUV spectra were observed by IUVS at Mars (Fig. 1). The hallmark of an aurora is the presence of dayside spectroscopic features in selected nightside spectra—in this case, the CO Cameron bands, the $CO_2^+$ ultraviolet doublet (UVD), and oxygen 297-nm emission (*19*). All emissions ultimately arise from the dissociation and ionization of $CO_2$, the dominant gas in Mars' atmosphere. In the absence of sunlight, energetic particle excitation is required to produce the emissions. No auroral emission has been detected in the FUV wavelength range, though the search for weak spectral features is ongoing. The auroral emissions are ~100 times weaker than their dayglow counterparts.

Contemporaneous time series for IUVS auroral brightnesses and electron fluxes measured by MAVEN's Solar Energetic Particle (SEP) (*20*) and Solar Wind Electron Analyzer (SWEA) (*21*) instruments show correlated behavior (Fig. 2). Electron fluxes as a function of energy were derived from 3- to 4-keV measurements (SWEA) and from 25- to 200-keV measurements (SEP). The particle data in the bottom three panels of Fig. 2 show quiescent

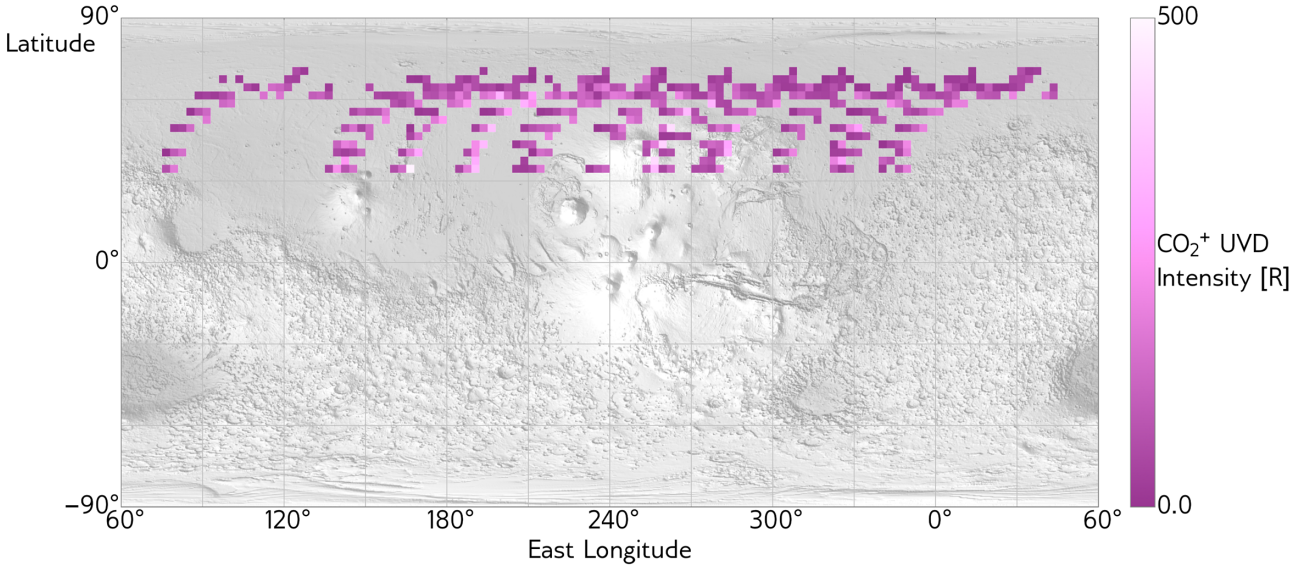


**Fig. 3. Geographic distribution of auroral emission.** $CO_2^+$ UVD emission brightnesses superposed on a map of Mars. The extent of emission was limited by the regions observed rather than the occurrence of auroras. All observations were obtained along the same nightside orbit path evident in the pattern of parallel arcs sloping up to the right. Geographic coverage was obtained by the rotation of the planet underneath on subsequent orbits, with longitudes shifting ~66° westward every orbit. It is possible that a large fraction of the nightside exhibited auroral emission during this period.

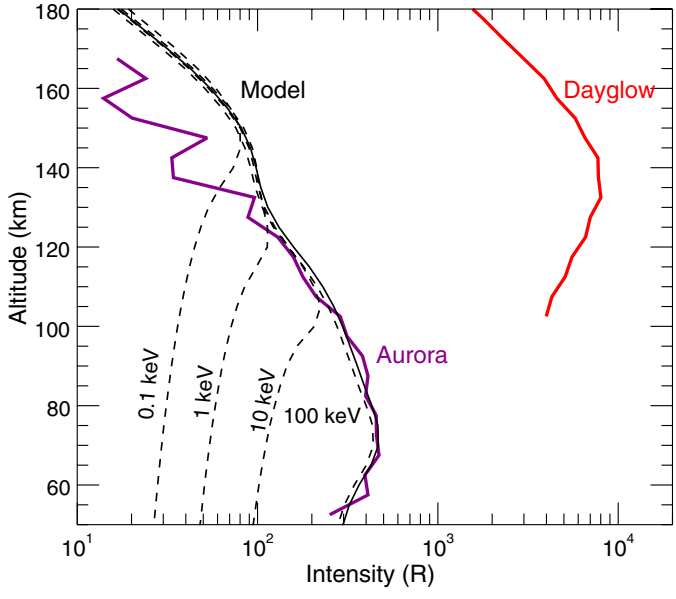


**Fig. 4. Observed and modeled vertical brightness profiles for auroral emission.** The red curve denotes the $CO_2^+$ UVD in daylight near the terminator; the purple curve indicates the $CO_2^+$ UVD during auroras on the nightside. Whereas the photons that excite UVD emission on the dayside are absorbed at altitudes between 120 and 150 km (depending on solar zenith angle), the energetic electrons that excite auroral emission penetrate nearly 60 km lower. The black curve shows the model emission profiles based on the SEP and SWEA data. Dashed lines show truncated energy distributions to illustrate how the maximum energy controls the depth of penetration.

behavior up until 17 December 2014. In the following hours, the solar energetic particle flux increases by two orders of magnitude, and electrons are clearly detected up to the 200-keV limit of the instrument. Data from SWEA measurements also show a comparable rise. Note that when corrected for scale differences and reduced solar energetic particle sensitivity at low energies, the energy distribution decreases smoothly and monotonically over four orders of magnitude. The lack of any peak at intermediate energies is an indication that no local acceleration has occurred. The auroral intensities in the top panel of Fig. 2 follow the same temporal behavior, lasting through the end of the IUVS observations in that period on 23 December. Note that although the onset, rise, and decay of the solar energetic particles and auroral phenomena are consistent, there are clear differences in the detailed structure of the time series. These differences could stem from short-term variability on the 10-min observations for IUVS or spatial structures in either the aurora or particle environment. The correlation between solar energetic particle events and auroral emission is confirmed by at least three additional occurrences observed in February and March 2015 (*22*).

Auroral emissions were detected in all 17 periapse passes during the 5-day period of solar energetic particle enhancement in December 2014, as well as in 97% of 120 vertical scans with appropriate geometry within those passes. The spatial distribution of auroral emission recorded in IUVS observations spanned ~35° in latitude and did not reach Mars' southern hemisphere (Fig. 3). It is probable that the aurora was even more geographically widespread than the large region observed. There is apparently no correlation between the geographic location of the aurora and its brightness. It is possible, however, that local time plays a role in controlling emission. IUVS only sampled a limited range on the nightside, with a relatively fixed ground track during this period from 35°N and ~00:30 local time to 70°N and 5:00 local time. Diffuse emission detected in March 2015 (*23*) occurred near the evening terminator; this finding suggests that narrow confinement in local time is unlikely.

The vertical profile of auroral emission in Mars' atmosphere offers important insights into the deposition of particle energy. The observed average vertical emission profile (Fig. 4) shows a broad emission peak at an apparent altitude of 70 km. This altitude could be interpreted as either the true altitude of emission at the limb or a geometrically projected value for higher-altitude auroras in front of or behind the limb. The latter was the case for SPICAM observations (*4*–*7*), as small patches observed infrequently were unlikely to appear at the limb of the planet. In the IUVS case, the presence of emission at all observed locations and over 5 days continuously provides evidence against substantial patchiness, and the consistency of widely separated individual altitude profiles suggests that projection effects in front of or behind the limb are not important.

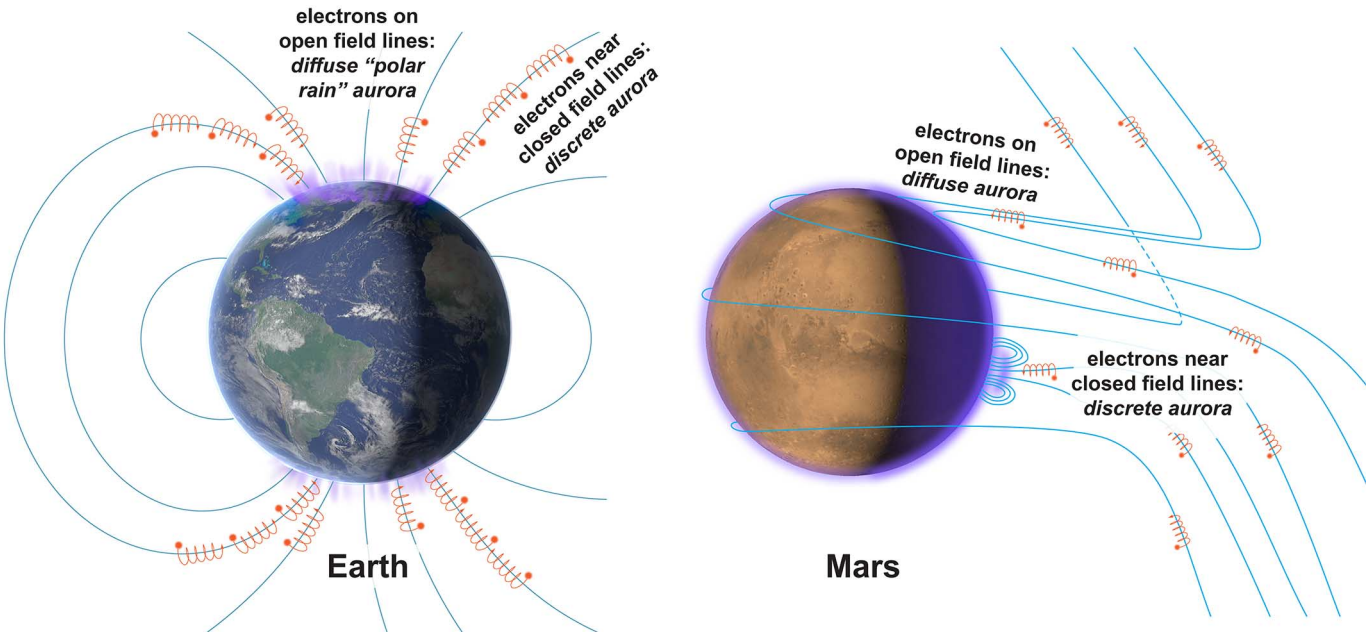


**Fig. 5. Comparison of field geometry for diffuse and discrete auroras on Earth and Mars.** Mars lacks an internally generated global magnetic field, due to the cooling of its core. Fields surrounding Mars are a combination of small structures locked in the crust billions of years ago (lower right) and solar wind field lines draped around the planet.

The 70-km altitude of the emission peak is compelling evidence for very-high-energy particle precipitation. Both dayglow and SPICAM auroral emissions peak ~60 km higher, where the pressure is lower by a factor of ~$10^4$. The IUVS aurora must therefore be excited by particles penetrating much deeper than the EUV photons responsible for the airglow or the <1-keV electrons typically responsible for the SPICAM aurora.

Modeling of the auroral emission profile confirms that the energetic particle population detected by SEP and SWEA can produce the observed low-altitude emission peak. As a representative spectrum, we used SEP and SWEA measurements at an altitude of 400 km from the outbound portion of orbit 437. We use SWEA data over its entire energy range from 3 to 5 keV. We then use a power law interpolation between 5 keV and the higher-energy electron spectra measured by SEP from 30 to 200 keV. The overall distribution approximately follows a power law of index 2.2 from ~10 to 200 keV.

We used the Boltzmann three-constituent (B3C) model (*24*) to solve the Boltzmann transport equation for energetic electrons. The B3C model has been used to study the FUV airglow from Earth (*22*, *25*, *26*), Titan (*27*), and Triton (*28*). For the purposes of our study, we adapted this model to the martian atmosphere. The B3C model degrades the energy of the electrons through dissociation, ionization, excitation, and other energy-loss processes and allows us to calculate an omnidirectional vertical electron flux (in units of centimeters$^{-2}$ second$^{-1}$ electron volt$^{-1}$). The electron flux is then used as input to the Atmospheric Ultraviolet Radiance Integrated Code (AURIC), which was originally developed for terrestrial use (*29*) and recently adapted for use at Mars (*30*), to calculate volume emission rates and column emission rates. Inputs to the B3C model include a mean martian neutral atmosphere (consisting of $CO_2$, $N_2$, and O) based on the Mars Climate Database (*31*).

The shape of the emission profile predicted from the full SEP and SWEA electron distributions (black line in Fig. 4) is a good match to the observations. (The measured energy flux has been scaled to match the model-predicted peak UVD brightness to the peak brightness measured by IUVS; future modeling work will be required to confirm the absolute brightness.) The dashed lines in Fig. 4 show the cumulative contributions found by truncating the energy distributions at increasing energies. These energy-dependent profiles demonstrate that electrons with energies less than ~100 eV interact strongly with atmospheric gases through ionization and excitation and are stopped at relatively high altitudes. The ~140-km inflection at this energy is close to the altitude for the lower-energy aurora observed by SPICAM. At high energies, the cross section for interaction decreases, and the particles penetrate deeper. Ultimately, the highest-energy incident electrons create a multitude of secondary electrons at lower energies and altitudes, which efficiently interact with the local gases to cause further ionization and excitation. Only a sufficiently "hard" electron energy distribution, with substantial fluxes of electrons with energies up to at least ~200 keV, can create a single dominant peak at 70 km.

## Discussion and conclusions

The discovery of diffuse low-altitude auroras on Mars allows a more complete comparison of auroral phenomena between Mars and Earth (Fig. 5), dictated by their very different magnetic field configurations. The critical distinction lies between field lines that are "closed," meaning connected to the planet on both ends, versus "open" or "draped," with at least one end not connected to the planet. Discrete auroras occur at Earth in the auroral ovals along the edges of closed field lines, where the interaction between Earth's magnetic field and the solar wind accelerates magnetospheric particles to sufficient energies to cause auroras. A similar interaction probably occurs at Mars to cause discrete auroras. Where crustal fields are present, their complex rotating interaction with the variable solar wind allows opportunities for particle acceleration. Over discrete auroras, Mars Express observed particle populations that had been accelerated to energies up to 100 eV, though the local acceleration mechanism remains unclear. Thus, Earth's auroral ovals and Mars' discrete auroral patches probably originate from analogous processes, despite their different appearances.

Diffuse auroras occur differently on the two planets as well. Terrestrial polar rain aurora and the Mars diffuse aurora are both powered by electrons accelerated at the Sun and not locally at the planet. (We note again that Earth's diffuse auroras, which occur deep within the magnetosphere, have no direct counterpart on Mars, so we do not discuss them here.) Electrons can directly collide with Earth's atmosphere along open field lines poleward of the auroral ovals and can strike Mars' atmosphere away from strong closed crustal magnetic fields. Mars' field lines, which are open or draped, allow solar energetic particles to penetrate the atmosphere during solar storms. These particles, which are 100 to 1000 times more energetic than those causing discrete auroras, reach much lower altitudes in the atmosphere. Open and draped field lines often cover much of the planet, though the locations change

as the planet rotates in the variable solar wind (*32*). Mars distorts the solar wind magnetic field, draping field lines that thread through much of the planet's atmosphere, including the nightside (Fig. 5). Diffuse auroras on Mars could therefore occur practically anywhere, and potentially nearly everywhere, on the planet.

The Mars diffuse aurora has much in common with auroras on Venus and some moons of the Jovian planets. Diffuse auroras are not surprising at Venus, which has neither a global magnetic field nor any crustal fields. The Pioneer Venus orbiter first detected auroras from oxygen emission at 130-nm UV wavelengths, where the auroras were attributed to relatively low-energy electrons (*33*, *34*). (No such emission was detected in IUVS observations at Mars.) Venus auroras have also been detected at visible wavelengths through ground-based observations, where they might be caused by solar energetic particles (*35*, *36*), as in this work. Analogously, Jupiter's moons Io and Europa lack intrinsic magnetic fields. In their cases, their tenuous atmospheres are exposed to the energetic particle population of the jovian magnetosphere within which they are embedded. The resulting particle-generated auroral emissions are more globally distributed, and the particles are not locally accelerated (*37*). Enabled by MAVEN and IUVS, the study of Mars' diffuse auroras may therefore have applications to these other solar system objects and potentially also to extrasolar planets without intrinsic magnetic fields.

Diffuse auroras may have additional effects on atmospheric processes. Only a fraction of the deposited energy results in atmospheric excitation and emission. Incident particles also ionize and dissociate atmospheric species, as well as heat the target atmosphere. These effects can lead to increased atmospheric escape rates: Ionized particles at sufficient altitudes can escape via outflow processes, and atmospheric heating can lead to increased thermal escape. Detailed modeling is required to estimate the extent to which atmospheric escape rates increase during diffuse auroral events, as well as which species escape more efficiently. The knowledge that auroras can occur on a more global scale at Mars lends new importance to these studies.

## REFERENCES AND NOTES


1. P. E. Sandholt, H. C. Carlson, A. Egeland, *Dayside and Polar Cap Aurora* (Kluwer Academic Publishers, Dordrecht, Netherlands, 2002).
2. P. T. Newell, T. Sotirelis, S. Wing, Diffuse, monoenergetic, and broadband aurora: The global precipitation budget. *J. Geophys. Res.* **114**, A09207 (2009) and references therein.
3. Y. Zhang, L. J. Paxton, A. T. Y. Lui, Polar rain aurora. *Geophys. Res. Lett.* **34**, L20114 (2007). doi: 10.1029/2007GL031602
4. M. H. Acuña *et al*., Global distribution of crustal magnetization discovered by the Mars Global Surveyor MAG/ER experiment. *Science* **284**, 790–793 (1999). doi: 10.1126/science.284.5415.790; pmid: 10221908
5. J.-L. Bertaux *et al*., Discovery of an aurora on Mars. *Nature* **435**, 790–794 (2005). doi: 10.1038/nature03603; pmid: 15944698
6. F. Leblanc *et al*., Origins of the martian aurora observed by Spectroscopy for Investigation of Characteristics of the Atmosphere of Mars (SPICAM) on board Mars Express. *J. Geophys. Res.* **111**, A09313 (2006). doi: 10.1029/2006JA011763
7. F. Leblanc *et al*., Observations of aurorae by SPICAM ultraviolet spectrograph on board Mars Express: Simultaneous ASPERA-3 and MARSIS measurements. *J. Geophys. Res.* **113**, A08311 (2008). doi: 10.1029/2008JA013033
8. J.-C. Gérard *et al*., Concurrent observations of ultraviolet aurora and energetic electron precipitation with Mars Express. *J. Geophys. Res.* **120**, 6749–6765 (2015). doi: 10.1002/2015JA021150
9. R. Lundin *et al*., Plasma acceleration above martian magnetic anomalies. *Science* **311**, 980–983 (2006). doi: 10.1126/science.1122071; pmid: 16484488
10. D. A. Brain *et al*., On the origin of aurorae on Mars. *Geophys. Res. Lett.* **33**, L01201 (2006). doi: 10.1029/2005GL024782
11. J. L. Fox, J. F. Brannon, H. S. Porter, Upper limits to the nightside ionosphere of Mars. *Geophys. Res. Lett.* **20**, 1339–1342 (1993). doi: 10.1029/93GL01349
12. F. Leblanc, J. G. Luhmann, R. E. Johnson, E. Chassefiere, Some expected impacts of a solar energetic particle event at Mars. *J. Geophys. Res.* **107**, 1058 (2002). doi: 10.1029/2001JA900178
13. R. J. Lillis, D. A. Brain, Nightside electron precipitation at Mars: Geographic variability and dependence on solar wind conditions. *J. Geophys. Res.* **118**, 3546–3556 (2013). doi: 10.1002/jgra.50171
14. B. Jakosky *et al*., The Mars Atmosphere and Volatile Evolution (MAVEN) mission. *Space Sci. Rev.* 10.1007/s11214-015-0139-x (2015). doi: 10.1007/s11214-015-0139-x
15. W. E. McClintock *et al*., The Imaging Ultraviolet Spectrograph (IUVS) for the MAVEN Mission. *Space Sci. Rev.* 10.1007/s11214-014-0098-7 (2014). doi: 10.1007/s11214-014-0098-7
16. M. Snow, A. Reberac, E. Quémerais, J. Clarke, W. E. McClintock, T. N. Woods, "A new catalog of ultraviolet stellar spectra for calibration," in *Cross-Calibration of Far UV Spectra of Solar System Objects and the Heliosphere*, E. Quémerais, M. Snow, R.-M. Bonnet, Eds. (ISSI Scientific Report Series, Springer, New York, 2013), pp. 191–226.
17. M. H. Stevens *et al*., New observations of molecular nitrogen in the martian upper atmosphere by IUVS on MAVEN. *Geophys. Res. Lett.* 10.1002/2015GL065319 (2015).
18. M. H. Stevens *et al*., The production of Titan's ultraviolet nitrogen airglow. *J. Geophys. Res.* **116**, A05304 (2011). doi: 10.1029/2010JA016284
19. S. K. Jain *et al*., The structure and variability of Mars upper atmosphere as seen in MAVEN/IUVS dayglow observations. *Geophys. Res. Lett.* 10.1002/2015GL065419 (2015).
20. D. E. Larson, R. J. Lillis, P. A. Dunn, A. Rahmati, T. E. Cravens, K. Hatch, M. Robinson, D. Glaser, J. Chen, D. W. Curtis, C. Tiu, R. P. Lin, J. G. Luhman, J. P. McFadden, J. Connerney, J. Halekas, B. M. Jakosky, "The Solar Energetic Particle experiment on MAVEN: First results," in *46th Lunar and Planetary Science Conference* (Lunar and Planetary Institute, Houston, TX, 2015), abstract 2890.
21. D. L. Mitchell, C. Mazelle, J. P. McFadden, D. Larson, J. S. Halekas, J. E. P. Connerney, J. Espley, L. Andersson, J. G. Luhmann, R. J. Lillis, M. Fillingim, T. Hara, D. A. Brain, "MAVEN observations of the martian ionosphere and magneotheath [sic]," in *46th Lunar and Planetary Science Conference* (Lunar and Planetary Institute, Houston, TX, 2015), abstract 3015.
22. D. J. Strickland, J. R. Jasperse, J. A. Whalen, Dependence of auroral FUV emissions on the incidence electron spectrum and neutral atmosphere. *J. Geophys. Res.* **88**, 8051–8062 (1983). doi: 10.1029/JA088iA10p08051
23. B. M. Jakosky *et al*., MAVEN observations of the response of Mars to an interplanetary coronal mass ejection. *Science* **350**, aad0210 (2015).
24. D. J. Strickland, D. L. Book, T. P. Coffey, J. A. Fedder, Transport equation techniques for the deposition of auroral electrons. *J. Geophys. Res.* **81**, 2755–2764 (1976). doi: 10.1029/JA081i016p02755
25. D. J. Strickland, R. R. Meier, J. H. Hecht, A. B. Christensen, Deducing composition and incident electron spectra from ground-based auroral optical measurements: Theory and model results. *J. Geophys. Res.* **94**, 13527–13539 (1989). doi: 10.1029/JA094iA10p13527
26. J. S. Evans *et al*., Ultraviolet plume instrument imaging from the LACE satellite: Analysis of broadband UV auroral limb data. *J. Geophys. Res.* **99**, 17591–17600 (1994). doi: 10.1029/94JA01143
27. D. F. Strobel, R. R. Meier, M. E. Summers, D. J. Strickland, Nitrogen airglow sources: Comparison of Triton, Titan, and Earth. *Geophys. Res. Lett.* **18**, 689–692 (1991). doi: 10.1029/91GL00133
28. D. F. Strobel, M. E. Simmers, F. Herbert, B. R. Sandel, The photochemistry of methane in the atmosphere of Triton. *Geophys. Res. Lett.* **17**, 1729–1732 (1990). doi: 10.1029/GL017i010p01729
29. D. J. Strickland *et al*., Atmospheric Ultraviolet Radiance Integrated Code (AURIC): Theory, software architecture, inputs, and selected results. *J. Quant. Spectrosc. Radiat. Transf.* **62**, 689–742 (1999). doi: 10.1016/S0022-4073(98)00098-3
30. J. S. Evans *et al*., Retrieval of CO2 and N2 in the martian thermosphere using dayglow observations by IUVS on MAVEN. *Geophys. Res. Lett.* 10.1002/2015GL065489 (2015).
31. E. Millour, F. Forget, A. Spiga, T. Navarro, J.-B. Madeleine, L. Montabone, F. Lefevre, J.-Y. Chaufray, M. A. Lopez-Valverde, F. Gonzalez-Galindo, S. R. Lewis, P. L. Read, M.-C. Desjean, J.-P. Huot; the MCD/GCM Development Team, "The Mars Climate Database, MCD version 5.1," in *Eighth International Conference on Mars* (Lunar and Planetary Institute, Houston, TX, 2014), no. 1791, p. 1184.
32. D. A. Brain, R. J. Lillis, D. L. Mitchell, J. S. Halekas, R. P. Lin, Electron pitch angle distributions as indicators of magnetic field topology near Mars. *J. Geophys. Res.* **112**, A09201 (2007). doi: 10.1029/2007JA012435
33. J. L. Phillips, A. I. F. Stewart, J. G. Luhmann, The Venus ultraviolet aurora: Observations at 130.4 nm. *Geophys. Res. Lett.* **13**, 1047–1050 (1986). doi: 10.1029/GL013i010p01047
34. J. Fox, A. I. F. Stewart, The Venus ultraviolet aurora: A soft electron source. *J. Geophys. Res.* **96**, 9821–9828 (1991). doi: 10.1029/91JA00252
35. T. G. Slanger, D. L. Huestis, P. C. Cosby, N. J. Chanover, T. A. Bida, The Venus nightglow: Ground-based observations and chemical mechanisms. *Icarus* **182**, 1–9 (2006). doi: 10.1016/j.icarus.2005.12.007
36. C. L. Gray, thesis, New Mexico State University (2015).
37. M. A. McGrath, E. Lellouch, D. F. Strobel, P. D. Feldman, R. E. Johnson, "Satellite atmospheres," in *Jupiter: The Planet, Satellites and Magnetosphere*, F. Bagenal, T. E. Dowling, W. B. McKinnon, Eds. (Cambridge Planetary Science Series, Cambridge Univ. Press, Cambridge, 2004), pp. 457–484.
38. J.-L. Bertaux *et al*., Nightglow in the upper atmosphere of Mars and implications for atmospheric transport. *Science* **307**, 566–569 (2005). doi: 10.1126/science.1106957; pmid: 15681381
39. A. Stiepen, A. I. F. Stewart, S. K. Jain, N. M. Schneider, J. Deighan, J. S. Evans, M. H. Stevens, F. Montmessin, M. S. Chaffin, W. E. McClintock, J. T. Clarke, G. M. Holsclaw, B. M. Jakosky, "Preliminary analysis of martian nightglow and aurora observed by MAVEN's Imaging Ultraviolet Spectrograph," in *46th Lunar and Planetary Science Conference* (Lunar and Planetary Institute, Houston, TX, 2015), abstract 2937.


## ACKNOWLEDGMENTS


The MAVEN mission is supported by NASA through the Mars Exploration Program. A.S. was supported by the Belgian American Educational Foundation and the Rotary District 1630. M.H.S. was supported by the NASA MAVEN Participating Scientist Program. This work was partially supported by the Centre National d'Etudes Spatiales, for the part based on observations with the SWEA instrument. The IUVS data are publicly archived at the Planetary Atmospheres node of the Planetary Data System and can be identified by the file suffix v03_r01.

17 July 2015; accepted 21 September 2015
10.1126/science.aad0313

**Discovery of diffuse aurora on Mars**

N. M. Schneider *et al.*

*Science* **350**, (2015);
DOI: 10.1126/science.aad0313